

# Mathematical characterization of the compression of granular materials

Eulalio Juárez-Badillo  
 Graduate School of Engineering, National University of Mexico



## ABSTRACT

The general theoretical equations of compressibility for geomaterials given by the Principle of Natural Proportionality are applied and described successfully all the experimental curves of compression of granular materials contained in the basic paper by Mesri and Vardhanabhuti (Can. Geotech. J. 46: 369 392, 2009).

## RESUMEN

Se aplicaron las ecuaciones teóricas generales que proporciona el principio de proporcionalidad natural, para describir exitosamente todas las curvas de compresión experimentales de materiales granulares contenidas en el artículo de Mesri y Vardhanabhuti (Can. Geotech. J. 46: 369 392, 2009).

## 1 INTRODUCTION

“Compression of granular materials” is the title of a paper by Gholamreza Mesri and Barames Vardhanabhuti published in the Canadian Geotechnical Journal in April, 2009, 46: 369 392.

After reading this paper the author was highly motivated to apply the theoretical equations of compressibility given by the principle of natural proportionality to the experimental data contained in it. The result is the subject of this paper.

## 2 THEORETICAL EQUATIONS

The theoretical equations of compressibility are (Juárez-Badillo 1981):

For the unvirgin zone:

$$V = \frac{V_0}{1 + \left(\frac{\sigma}{\sigma^*}\right)^{\gamma_u}} \quad [1]$$

where  $V$  = volumen,  $\sigma$  = pressure,  $V_0 = V$  at  $\sigma = 0$ ,  $\sigma^*$  = characteristic  $\sigma$  at  $V = (1/2)V_0$  and  $\gamma_u$  = natural unvirgin coefficient of compressibility. For the virgin zone where  $V_0 = \infty$  at  $\sigma = 0$  Equation [1] reduces to

$$V = V_1 \left(\frac{\sigma}{\sigma_1}\right)^{-\gamma} \quad [2]$$

where  $(\sigma_1, V_1)$  is a known point and  $\gamma$  = natural virgin coefficient of compressibility.

In terms of void ratio  $e$ , Equations [1] and [2] read:

$$e = \frac{1 + e_0}{1 + \left(\frac{\sigma}{\sigma^*}\right)^{\gamma_u}} - 1 \quad [3]$$

$$e = (1 + e_1) \left(\frac{\sigma}{\sigma_1}\right)^{-\gamma} - 1 \quad [4]$$

## 3 PRACTICAL APPLICATION

Theoretical Equations [3] and [4] were applied to the experimental curves in the 23 Figures of the paper that contain such experimental curves (Figures 1 to 23). All parameter values are shown in each figure and also in Table 1.

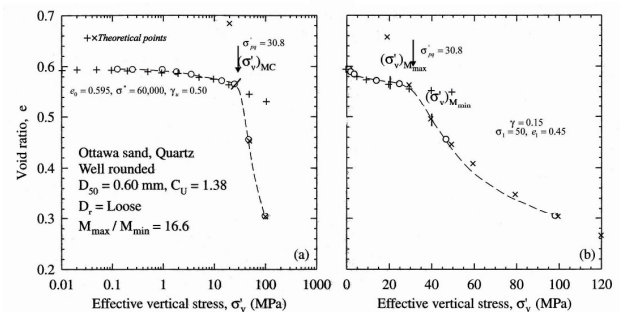


Figure 1. A compression behavior of a loose Ottawa sand. (data from Roberts and de Souza 1985)  $C_u$ , uniformity coefficient;  $D_r$ , relative density;  $D_{50}$ , mean grain size;  $M_{max}$ , tangent constrained modulus at the first inflection point;  $M_{min}$ , tangent constrained modulus at the second inflection point;  $(\sigma'_v)_{M_{max}}$ , effective vertical stress at the yield point defined at the first inflection point;  $(\sigma'_v)_{M_{min}}$ , effective vertical stress at the yield point defined at the second inflection point;  $(\sigma'_v)_{MC}$ , effective vertical stress at yield point defined at the point of maximum curvature

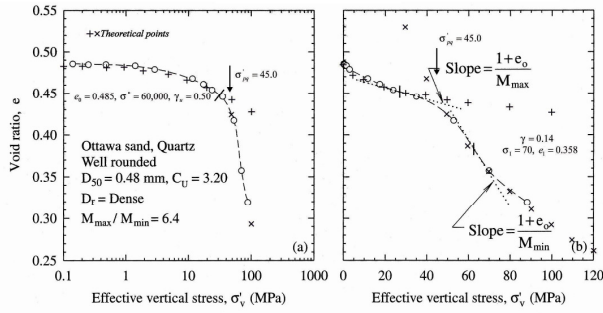


Figure 2. Type A compression behaviour of a dense Ottawa sand (data from Roberts and de Souza. 1958)  $e_0$ , initial void ratio

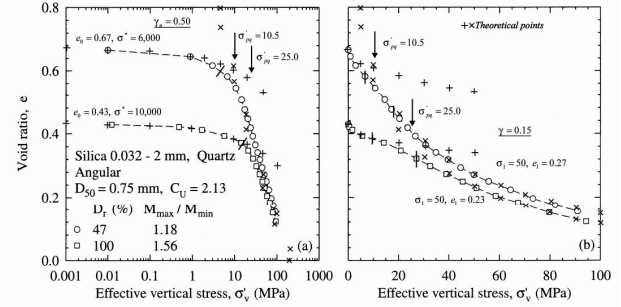


Figure 6. Type A compression behavior of quartz sand (data from Nakata et al. 2001b)

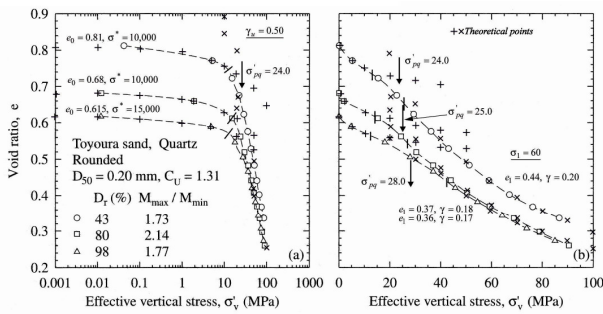


Figure 3. Type A compression behavior of Toyoura sand (data from Nakata et al. 2001a)

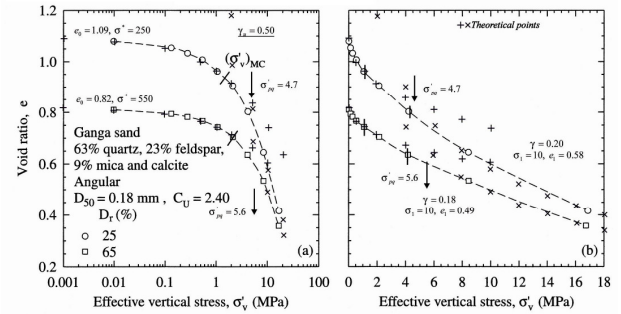


Figure 7. Type B compression behavior of Ganga sand (data from Rahim. 1989)

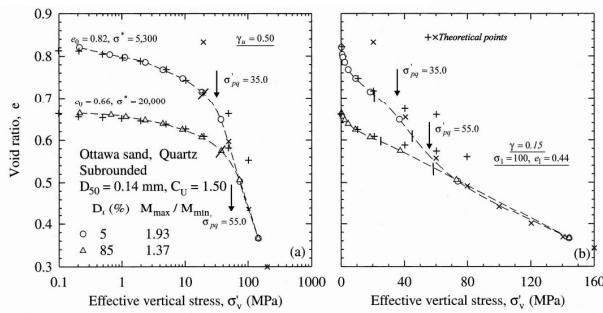


Figure 4. Type A behavior of Ottawa sand (data from Pestana and Whittle. 1995)

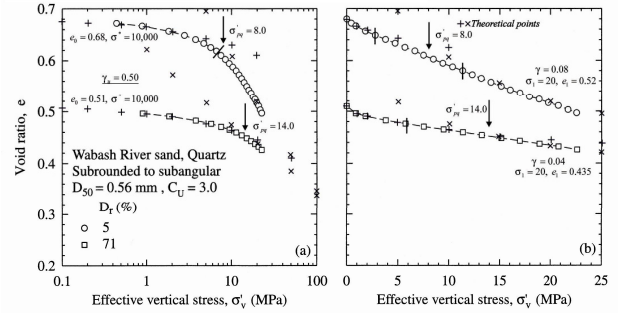


Figure 8. Type B compression behavior of Wabash River sand (data from Hendron. 1963)

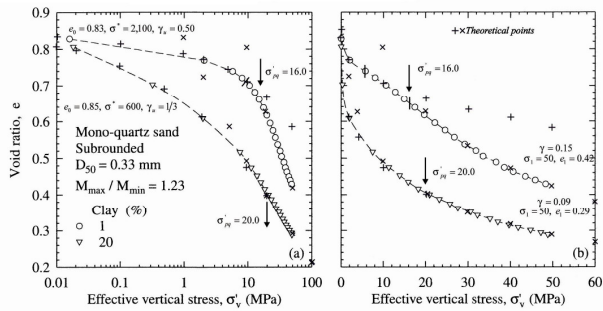


Figure 5. Type A compression behavior of mono-quartz sand (data from Chuhan et al. 2003)

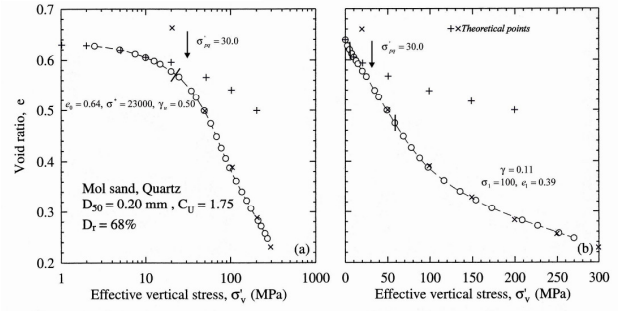


Figure 9. Type B compression behavior of Mol sand (data from DeBeer. 1963)

Table 1. Parameter values of the theoretical equations of compressibility

| Fig. | Dr<br>(%)               | Unvirgin |            |                     | Virgin              |       |          | $\sigma'_{pq}$<br>(Mpa) |
|------|-------------------------|----------|------------|---------------------|---------------------|-------|----------|-------------------------|
|      |                         | $e_o$    | $\gamma_u$ | $\sigma^*$<br>(Mpa) | $\sigma_1$<br>(Mpa) | $e_1$ | $\gamma$ |                         |
| 1    | Loose                   | 0.595    | 0.5        | 60,000              | 50                  | 0.450 | 0.15     | 30.8                    |
| 2    | Dense                   | 0.485    | 0.5        | 60,000              | 70                  | 0.358 | 0.14     | 45                      |
| 3    | 43                      | 0.810    | 0.5        | 10,000              | 60                  | 0.440 | 0.20     | 24                      |
|      | 80                      | 0.680    | 0.5        | 10,000              | 60                  | 0.370 | 0.18     | 25                      |
|      | 98                      | 0.615    | 0.5        | 15,000              | 60                  | 0.360 | 0.17     | 28                      |
| 4    | 5                       | 0.820    | 0.5        | 5,300               | 100                 | 0.440 | 0.15     | 35                      |
|      | 85                      | 0.660    | 0.5        | 20,000              | 100                 | 0.440 | 0.15     | 55                      |
| 5    | Clay 1%                 | 0.830    | 0.5        | 2,100               | 50                  | 0.420 | 0.15     | 16                      |
|      | Clay 20%                | 0.850    | 1/3        | 600                 | 50                  | 0.290 | 0.09     | 20                      |
| 6    | 47                      | 0.670    | 0.5        | 6,000               | 50                  | 0.270 | 0.15     | 10.5                    |
|      | 100                     | 0.430    | 0.5        | 10,000              | 50                  | 0.230 | 0.15     | 25                      |
| 7    | 25                      | 1.090    | 0.5        | 250                 | 10                  | 0.580 | 0.20     | 4.7                     |
|      | 65                      | 0.820    | 0.5        | 550                 | 10                  | 0.490 | 0.18     | 5.6                     |
| 8    | 5                       | 0.680    | 0.5        | 10,000              | 20                  | 0.520 | 0.08     | 8                       |
|      | 71                      | 0.510    | 0.5        | 10,000              | 20                  | 0.435 | 0.04     | 14                      |
| 9    | 68                      | 0.640    | 0.5        | 23,000              | 100                 | 0.390 | 0.11     | 30                      |
| 10   | 5                       | 1.150    | 0.5        | 160                 | 100                 | 0.300 | 0.09     | 50                      |
| 11   | 40                      | 1.050    | 0.5        | 200                 | 50                  | 0.350 | 0.10     | 2                       |
|      | 88                      | 0.840    | 0.5        | 500                 | 50                  | 0.350 | 0.10     | 7                       |
| 12   | $D_{60}=0.19\text{mm}$  | 1.220    | 0.5        | 250                 | 20                  | 0.600 | 0.14     | 5                       |
|      | $D_{60}=1.48\text{ mm}$ | 1.270    | 0.5        | 130                 | 20                  | 0.490 | 0.14     | 2.5                     |
| 13   | 24                      | 0.990    | 0.5        | 90                  | -                   | -     | -        | >10                     |
| 14   | 5                       | 0.940    | 0.5        | 600                 | -                   | -     | -        | >50                     |
|      | 86                      | 0.760    | 0.5        | 1,800               | -                   | -     | -        | >50                     |
| 15   | 40                      | 0.990    | 0.5        | 60                  | 10                  | 0.180 | 0.28     | 3.25                    |
| 16   | 22                      | 0.690    | 1/3        | 1,400               | 50                  | 0.270 | 0.10     | 50                      |
|      | 100                     | 0.280    | 0.5        | 3,000               | 50                  | 0.150 | 0.10     | 70                      |
| 17   | 46                      | 0.850    | 0.5        | 60,000              | 200                 | 0.650 | 0.15     | 122                     |
|      | 54                      | 0.790    | 0.5        | 60,000              | 200                 | -     | -        | -                       |
|      | 80                      | 0.680    | 0.5        | 60,000              | 200                 | 0.550 | 0.07     | 122                     |
| 18   | 37                      | 0.815    | 2/3        | 1,000               | 30                  | 0.595 | 0.12     | 18                      |
|      | 52                      | 0.755    | 2/3        | 1,000               | 30                  | 0.555 | 0.12     | 20                      |
|      | 77                      | 0.660    | 2/3        | 3,000               | 30                  | 0.520 | 0.12     | 19                      |
| 19   | 5                       | 0.680    | 0.5        | 10,000              | 20                  | 0.515 | 0.08     | 8                       |
| 20   | 71                      | 0.510    | 0.5        | 11,000              | 20                  | 0.435 | 0.04     | 13                      |
| 21   | 63                      | 0.700    | 0.5        | 14,000              | 20                  | 0.580 | 0.13     | 14                      |
| 22   | 70                      | 0.680    | 0.5        | 20,000              | 20                  | 0.583 | 0.12     | 16                      |
| 23   | 89                      | 0.480    | 1/3        | $1.3 \times 10^6$   | 20                  | 0.440 | 0.01     | 7.5                     |

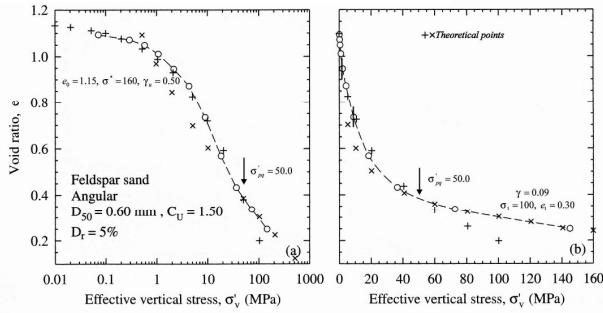


Figure 10. Type B compression behavior of Feldspar sand (data from Pestana and White. 1995)

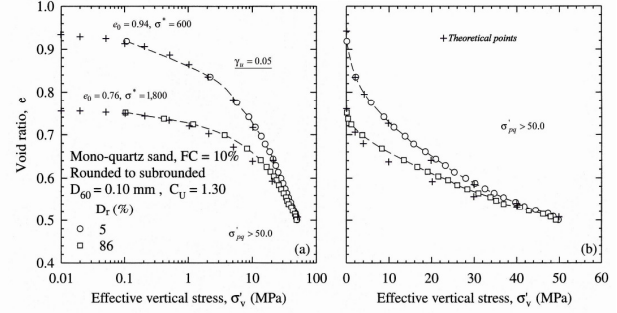


Figure 14. Type C compression behavior of mono-quartz sand (data from Chuhan et al. 2003)

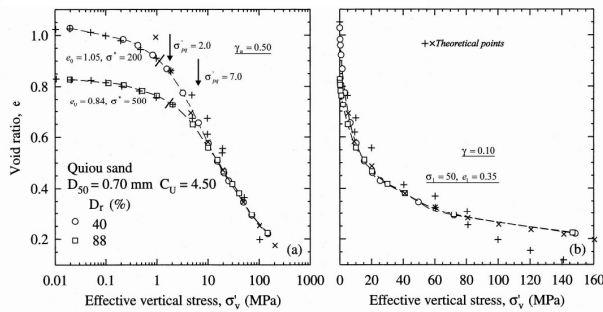


Figure 11. Type C compression behavior of Quiou sand (data from Pestana and White. 1995)

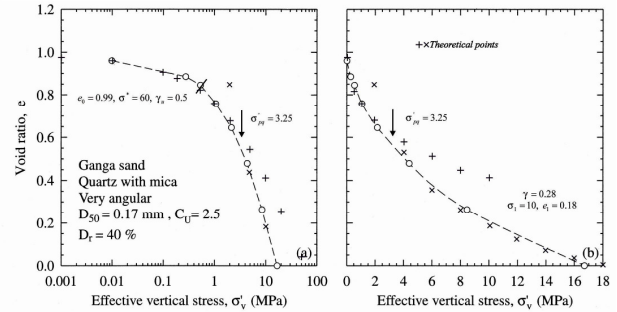


Figure 15. Type C compression behavior of Ganga sand (data from Rahim. 1989)

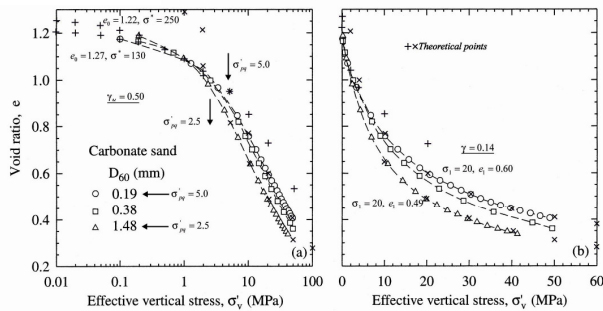


Figure 12. Type C compression behavior of carbonate sand (data from Chuhan. 2003). D<sub>60</sub>, grain size at which 60% if the sample is finer

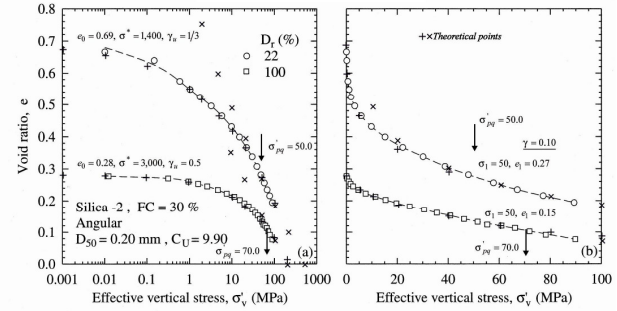


Figure 16. Type C compression behavior of silica-2 sand (data from Nakata et al. 2001b)

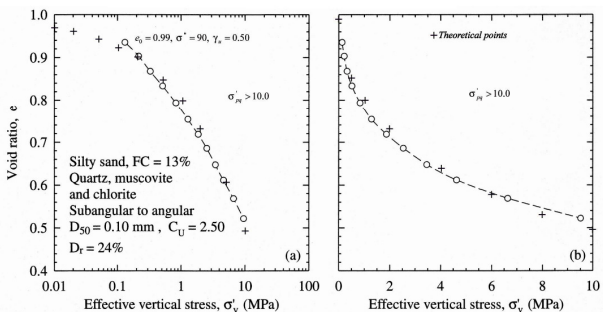


Figure 13. Type C compression behavior of silty sand (data from Huang et al. 1999). FC, fines content passing number 200 US standard sieve

The intersection of both equations, unvirgin and virgin, determine the theoretical quasi preconsolidation pressure  $\sigma'_{pq}$  in the material. The true preconsolidation pressure  $\sigma'_p$  is obtained with the virgin compression curve at  $t = \infty$ . In clays  $\sigma'_{pq}$  is obtained with the end of primary EOP curve and  $\sigma'_p$  is obtained with the end of secondary EOS curve (Juárez-Badillo et al. 2008).

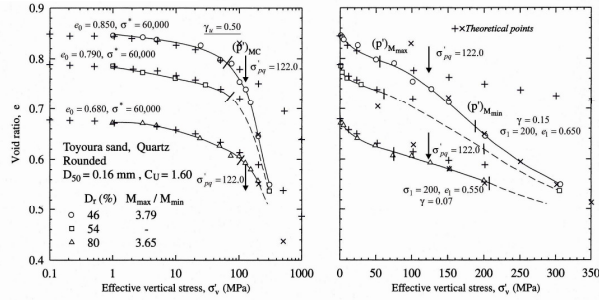


Figure 17. Type A compression behavior of Toyoura sand in isotropic compression (data from Kwag et al. 1999).  $(p)MC$ , equal all-around pressure at yield point defined at the point of maximum curvature of  $e$  versus  $\log p'$ ;  $(p)M_{max}$ , equal all-around pressure at yield point defined at first inflection point of maximum curvature of  $e$  versus  $\log p'$ ;  $(p)M_{min}$ , equal all-around pressure at the second inflection point of  $e$  versus  $p'$  defining end of the second stage of compression

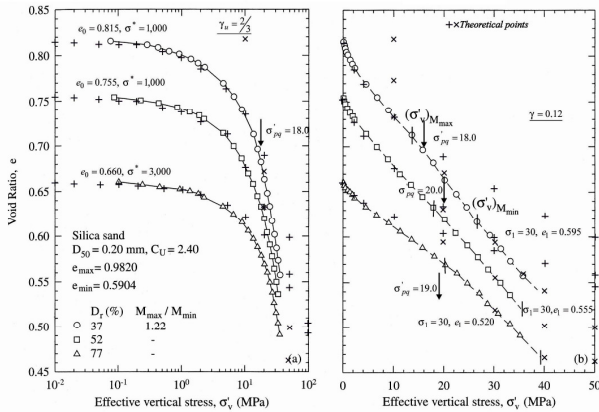


Figure 18. Compression behavior of Silica sand used to study secondary compression (data from Yet. 1998)

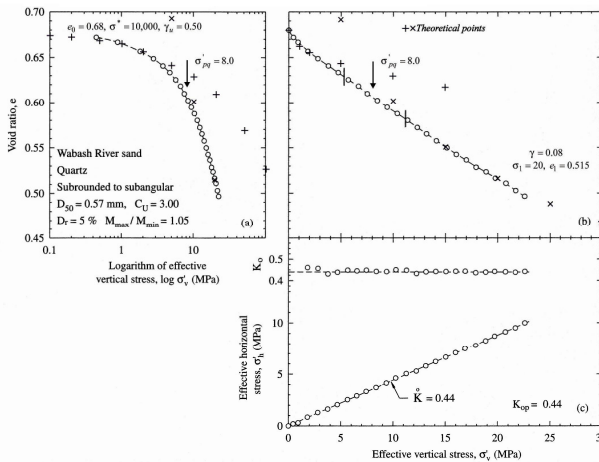


Figure 19. Behavior of  $K_0$  for normally consolidated young loose Wabash River sand with  $D_r = 5\%$  (data from Hendron. 1963).  $K$ , slope of  $\sigma'_h$  versus  $\sigma'_v = \Delta\sigma'_h/\Delta\sigma'_v$ ;

$K_{op}$ , coefficient of earth pressure at rest in normally consolidated young loose sand

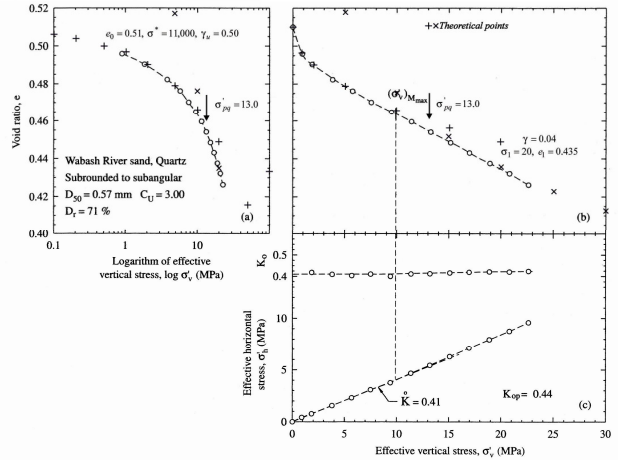


Figure 20. Compression behavior of  $K_0$  for normally consolidated young dense Wabash River sand with  $D_r = 71\%$  (data from Hendron. 1963)

Equations [1] and [2] have proven to describe the compressibility of all geomaterials: clays, sands, gravels, rocks and concrete (Juárez-Badillo. 1985) and also Equation [2] describes the compressibility of substances and liquids to pressures up to 45,000 kg/cm<sup>2</sup> if due account is taken of the constant internal pressure  $i$  characteristic of each substance and each liquid (Juárez-Badillo and Hernández-Mira 2006 a, b).

Clays, from its formation by self-weight consolidation behave with its virgin coefficient of consolidation  $\gamma$  in Equation [4], showing at the surface of the consolidation zone the electric chemical forces among clay particles of a magnitude of the order of 0.01 to 0.03 kPa (Juárez-Badillo 2008).

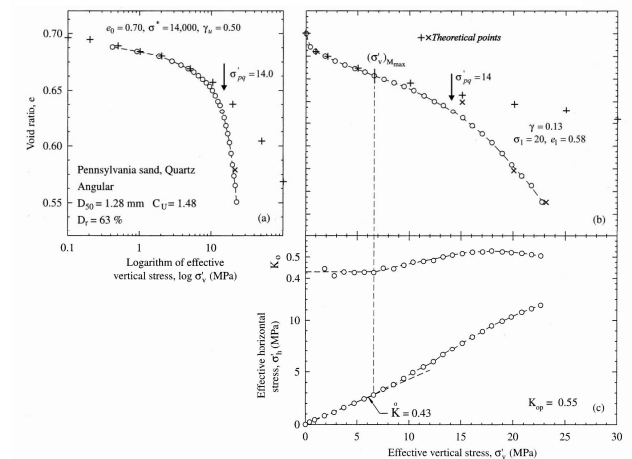


Figure 21. Behavior of  $K_0$  for normally consolidated young dense Pennsylvania sand with  $D_r = 63\%$  (data from Hendron. 1963)



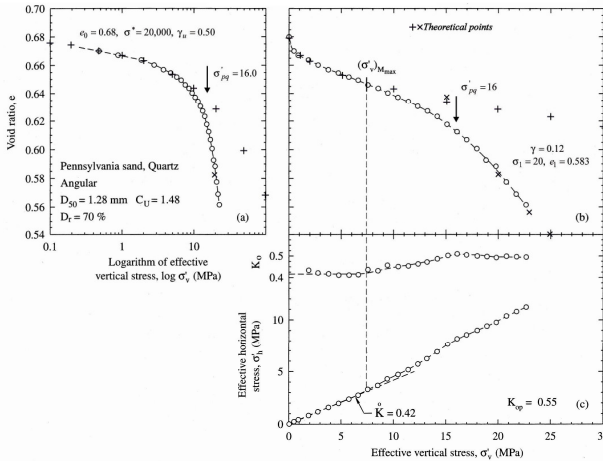


Figure 22. Behavior of  $K_0$  for normally consolidated young dense Pennsylvania sand with  $D_r = 74\%$  (data from Hendron. 1963)

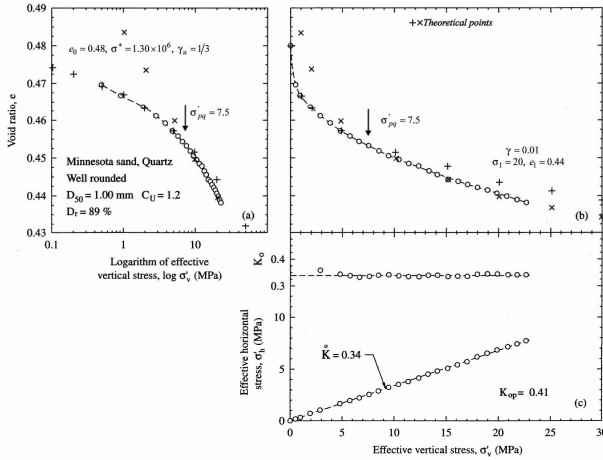


Figure 23. Behavior of  $K_0$  for normally consolidated young dense Minnesota sand with  $D_r = 89\%$  (data from Hendron. 1963)

#### 4 CONCLUSIONS

The theoretical equations of compressibility given by the Principle of Natural Proportionality describe successfully the experimental data of the 23 figures of compression of granular materials contained in the basic paper cited.

#### 5 ACKNOWLEDGMENT

The author is very grateful to Mrs. Juliana Constanza Zapata Chica and to Mr. Sergio Hernández Mira for the assistance in the preparation of this paper.

#### 6 REFERENCES

- Juárez-Badillo, E. 1981. General compressibility equation for soils. In *Proceedings of X International Conference on Soil Mechanics and Foundations Engineering*, Stockholm, pp. 171-178.
- Juárez-Badillo, E. 1985. General volumetric constitutive equation for geomaterials. Special volume in *Constitutive Laws of Soils*. In *Proceedings of XI International Conference on Soil Mechanics and Foundation Engineering*, San Francisco. Japanese Society for Soil Mechanics and Foundation Engineering, Tokyo, pp. 131-135.
- Juárez-Badillo, E. 2008. The principle of natural proportionality applied to self-weight consolidation. In *Proceedings of XXIV Reunión Nacional de Mecánica de Suelos*, Aguascalientes, México, pp. 335-337.
- Juárez-Badillo, E. and Hernández-Mira, S. 2006a. Mathematical characterization of the compression to 45,000 kg/cm<sup>2</sup> of fourteen substances. In *Proceedings of International Conference on New Developments in Geoenvironmental and Geotechnical Engineering*, Incheon, Korea, pp. 154-161.
- Juárez-Badillo, E. and Hernández-Mira, S. 2006b. Mathematical characterization of the compression to 40,000 kg/cm<sup>2</sup> of certain liquids. In *Proceedings of International Conference on New Developments in Geoenvironmental and Geotechnical Engineering*, Incheon, Korea, pp. 162-170.
- Juárez-Badillo, E., Aguirre-Menchana, L. M. and Zarate-Aquino, M. 2008. The theoretical quasi preconsolidation pressure in calys. In *Proceedings of XXIV Reunión Nacional de Mecánica de Suelos*, Aguascalientes, México, pp. 323-330.
- Mesri, G. and Vardhanabhuti, B. 2009. Compression of granular materials. *Canadian Geotechnical Journal*, 46(4): 369-392.